Mouse Bestrophin-2 Is a Bona fide Cl^- Channel: Identification of a Residue Important in Anion Binding and Conduction

Zhiqiang Qu, Rodolphe Fischmeister, and Criss Hartzell

Department of Cell Biology and The Center for Neurodegenerative Diseases, Emory University School of Medicine, Atlanta, GA 30322

ABSTRACT Bestrophins have recently been proposed to comprise a new family of Cl^- channels. Our goal was to test whether mouse bestrophin-2 (mBest2) is a bona fide Cl^- channel. We expressed mBest2 in three different mammalian cell lines. mBest2 was trafficked to the plasma membrane as shown by biotinylation and immunoprecipitation, and induced a Ca^{2+}-activated Cl^- current in all three cell lines (EC_{50} for Ca^{2+} = 230 nM). The permeability sequence was SCN^-: I^-: Br^-: Cl^-: F^- (8.2: 1.9: 1.4: 1: 0.5). Although SCN^- was highly permeant, its conductance was ~10% that of Cl^- and SCN^- blocked Cl^- conductance (IC_{50} = 12 mM). Therefore, SCN^- entered the pore more easily than Cl^-, but bound more tightly than Cl^-. Mutations in S79 altered the relative permeability and conductance for SCN^- as expected if S79 contributed to an anion binding site in the channel. P_{SCN}/P_{Cl} = 8.2 ± 1.3 for wild-type and 3.9 ± 0.4 for S79C. G_{SCN}/G_{Cl} = 0.14 ± 0.03 for wild-type and 0.94 ± 0.04 for S79C. In the S79 mutants, SCN^- did not block Cl^- conductance. This suggested that the S79C mutation altered the affinity of an anion binding site for SCN^-. Additional evidence that S79 was located in the conduction pathway was provided by the finding that modification of the sulfhydryl group in S79C with $MTSET^+$ or $MTSES^-$ increased conductance significantly. Because the effect of positively and negatively charged MTS reagents was similar, electrostatic interactions between the permeant anion and the channel at this residue were probably not critical in anion selectivity. These data provide strong evidence that mBest2 forms part of the novel Cl^- conduction pathway in mBest2-transfected cells and that S79 plays an important role in anion binding in the pore of the channel.

KEY WORDS: chloride channels • ion permeation • electrophysiology • mutagenesis • ion channel

INTRODUCTION

Recently, bestrophins have been proposed to be a new family of Cl^- channels (Sun et al., 2002; Qu and Hartzell, 2003; Tsunenari et al., 2003). A variety of evidence supports this suggestion. Mutations in human bestrophin-1 (hBest1) produce a disease called Best vitelliform macular dystrophy, which is a degeneration of the macular region (Petrukhin et al., 1998; Bakall et al., 1999; Caldwell et al., 1999; White et al., 2000). There have been suspicions that Best disease is caused by a Cl^- channel defect for some time. Best disease often develops in childhood and is associated with the accumulation of a yellow fluid between the retina and the retinal pigment epithelium (RPE) (Gass, 1987; O'Gorman et al., 1988). The fluid accumulation in Best disease is consistent with abnormal fluid transport, which often involves Cl^- channels. Furthermore, the characteristic diagnostic feature of this disease is a reduction in the amplitude of the slow light peak of the electro-oculogram (EOG) (Francois et al., 1967; Deutman, 1969). There is good evidence that the slow light peak is caused by a Cl^- conductance in the basolateral membrane of the RPE (Steinberg, 1985; Griff, 1991; Fujii et al., 1992; Bialek et al., 1995; Gallemore and Steinberg, 1993; Gallemore et al., 1998) and hBest1 has been shown by immunocytochemistry to be concentrated in this location (Marmorstein et al., 2000; Bakall et al., 2003). Finally, bestrophins from human, *C. elegans*, *Drosophila*, and *Xenopus* all induce Cl^- currents when expressed heterologously in HEK-293 cells (Qu and Hartzell, 2003; Sun et al., 2002). The I-V relationships and the rectification of the currents differ among the four bestrophins tested, but all appear to be Cl^- channels based on the dependence of the reversal potential on extracellular $[Cl^-]$ and sensitivity to the Cl^- channel blocker DIDS.

In addition to Best1, there are three other bestrophin genes in mammals (Stohr et al., 2002; Tsunenari et al., 2003). All four human bestrophins function as Cl^- channels when expressed in HEK-293 cells (Tsunenari et al., 2003), but whether mutations in bestrophins 2, 3, or 4 produce diseases is not known. Also, it is not known what specific roles these channels play in the physiology of specific tissues.

Address correspondence to Criss Hartzell, Department of Cell Biology and The Center for Neurodegenerative Diseases, 615 Michael St., 535 Whitehead Biomedical Research Building, Emory University School of Medicine, Atlanta, GA 30322-3030. Fax: (404) 727-6256; email: criss@cellbio.emory.edu

Abbreviations used in this paper: EOG, electro-oculogram; hBest1, human bestrophin-1; mBest2, mouse bestrophin-2; RPE, retinal pigment epithelium.

Although expression in HEK cells is a powerful tool for showing that a gene encodes an ion channel, this approach is not without pitfalls. In principle, expression of heterologous proteins could cause the up-regulation of an endogenous ion channel or could alter its trafficking to the plasma membrane. Such a phenomenon is well-documented in *Xenopus* oocytes, where expression of a wide variety of different membrane proteins, including nonconducting K^+ channel mutants, induces up-regulation of an endogenous current (see references in Kuruma et al., 2000). The goal of the present investigation was to test the hypothesis that mBest2 is involved in forming the pore of the novel Cl^- channel that is induced when cultured cells are transfected with mBest2 cDNA. We believe that three minimal conditions must be fulfilled in order to conclude that a mBest2 is a bona fide Cl^- channel. (a) mBest2 expression must produce identical Cl currents when expressed in different cell types. (b) The mBest2 protein must be expressed on the cell surface. (c) Mutations in putative pore domains of mBest2 must alter the conduction of anions through the expressed channels. Here we report that these three conditions are met. Most interestingly, we describe a mutation that produces significant changes in ion conduction through the channel. The nature of these changes suggests that this residue is involved in anion binding in the pore. These data provide substantial support for the idea that bestrophins are a new family of Cl^- channels and shed light on a residue in the protein that is important in regulating anion conduction.

MATERIALS AND METHODS

Heterologous Expression of mBest2 in Mammalian Cell Lines

Mouse Bestrophin-2 (mBest2) clone was obtained from the IMAGE collection at ATCC (IMAGE clone ID: 4989959; EMBL/GenBank/DDBJ accession no. BC031186 and NM_145388). The clone was sequenced to verify that its sequence agreed with the published EMBL/GenBank/DDBJ sequence. Cell lines used include HEK-293 (human embryonic kidney), ARPE-19 (human retinal pigment epithelium), and HeLa (human fibroblast). All cell lines were obtained from American Type Culture Collection.

mBest2 in pCMV-SPORT6 was transfected into HEK-293 cells along with a vector that expressed EGFP (pEGFP; Invitrogen) using Fugene-6 transfection reagent (Roche). To obtain modest amplitude of Ca^{2+}-activated Cl^- currents (1–2 nA per cell), 0.05–0.1 μg mBest2 cDNA was used to transfect one 35-mm culture dish. 1 d after transfection, cells were dissociated and replated on glass coverslips for electrophysiological recording. Transfected cells were identified by EGFP fluorescence and used for patch clamp experiments within 3 d after transfection.

Site-specific Mutagenesis of mBest2

Site-specific mutations were made using a PCR-based site-directed mutagenesis kit (Quickchange; Stratagene). Specific mutations were introduced into primers. The template, mBest2 in pCMV-SPORT6, was amplified with the primers and P*fu* DNA polymerase by the polymerase chain reaction. The original methylated templates were digested with Dpn-1 and the nonmethylated PCR products were transformed into XL-1 blue *E. coli*. Mutations were confirmed by DNA sequencing.

Electrophysiological Methods

Recordings were performed using the whole-cell recording configuration of the patch-clamp technique. Patch pipettes were made of borosilicate glass (Sutter Instrument Co.), pulled by a Sutter P-2000 puller (Sutter Instrument Co.), and fire-polished. Patch pipettes had resistances of 3–5 MΩ filled with the standard intracellular solution (see below). The bath was grounded via a 3-M KCl agar bridge connected to a Ag/AgCl reference electrode. Solution changes were performed by perfusing the 1-ml chamber at a speed of ~4 ml/min. To measure the steady-state current-voltage relationship, the cells were voltage clamped from a holding potential of 0 mV with 700-ms duration pulses from −100 mV to +100 mV in 20-mV increments. Because the currents were time independent, some experiments used 200-ms duration voltage ramps from −100 to +100 mV. Data were acquired by an Axopatch 200A amplifier controlled by Clampex 8.1 via a Digidata 1322A data acquisition system (Axon Instruments, Inc.). Experiments were conducted at room temperature (20–24°C). Liquid junction potentials were corrected using the liquid junction potential calculator in Clampex 8.1.

Solutions

The standard pipette solution contained (mM): 146 CsCl, 2 $MgCl_2$, 5 (Ca^{2+})-EGTA, 8 HEPES, 10 sucrose, pH 7.3, adjusted with NMDG. The "zero" Ca^{2+} pipette solution contained 5 mM EGTA without added Ca^{2+}, whereas the high Ca^{2+} pipette solution contained a mixture of 5 mM EGTA and 5 mM Ca^{2+}-EGTA to make solutions with different free [Ca^{2+}], as described by Tsien and Pozzan (Tsien and Pozzan, 1989; Kuruma and Hartzell, 2000). In the text, "high" Ca^{2+} solution refers to Ca^{2+} concentrations between 600 nM and 4.5 μM. The calculated Ca^{2+} concentrations were confirmed in each solution by fura-2 (Molecular Probes) measurements using an LS-50B luminescence spectrophotometer (Perkin Elmer). The standard extracellular solution contained (mM) 140 NaCl, 5 KCl, 2 $CaCl_2$, 1 $MgCl_2$, 15 glucose, 10 HEPES, pH 7.4 with NaOH. This combination of solutions set E_{rev} for Cl^- currents to zero, while cation currents carried by Na or Cs would have very positive or negative E_{rev}, respectively. When Cl^- was substituted with another anion, NaCl was replaced on an equimolar basis with NaX, where X is the substitute anion. Solution osmolarity was 303 mOsm for both intra- and extracellular solutions (Micro Osmometer, Model 3300; Advanced Instrument). Small differences in osmolarity were adjusted by addition of sucrose. For experiments with intracellular SCN^-, the pipette solution contained (mM) 140 NaSCN, 6 NaCl, 5 EGTA-Ca, 2 $MgCl_2$, 10 HEPES-Na, pH 7.3, and the extracellular solution contained 140 NaSCN (or NaCl), 2 NaCl, 2 $CaCl_2$, 2 $MgCl_2$, 10 HEPES-Na, pH 7.3. DIDS (Molecular Probes) was suspended in water at 50 mM as a stock before working solutions were made.

Sulfhydryl Modification

MTSET (2-trimethylammonioethylmethanethiosulfonate, bromide), MTSES [sodium (2-sulfonatoethyl) methanethiosulfonate], and MTSEA (2-aminoethylmethanethiosulfonate, hydrochloride) (Toronto Research Chemicals) were prepared in water, stored on ice, and used within 90 min. The standard extracellular solution with the reagents diluted to the indicated working concentration was made immediately before use.

Analysis of Data

For the calculations and graphical presentation, we used Origin 6.0 software (Microcal). Data is expressed as mean ± SEM. Rela-

tive permeability of the channels was determined by measuring the shift in E_{rev} upon changing the bath solution from one containing 151 mM Cl^- to another with 140 mM X and 11 mM Cl^-, where X is the substitute anion (Qu and Hartzell, 2000). The permeability ratio was estimated using the Goldman-Hodgkin-Katz equation.

$$P_X/P_{Cl} = [Cl^-]_i/\{[X]_o \exp(\Delta E_{rev}F/RT)\} - [Cl^-]_o/[X]_o,$$

where ΔE_{rev} is the difference between the reversal potential with the test anion X and that observed with symmetrical Cl^-, and F, R, and T have their normal thermodynamic meanings.

Biotinylation and Immunoprecipitation

All reactions were performed at 4°C. Nontransfected HEK-293 cells and HEK-293 cells transfected with mBest2 were placed on ice, washed three times with PBS, and biotinylated with 0.5 mg/ml Sulfo-NHS-LC Biotin (Pierce Chemical Co.) in PBS for 30 min. The cells were then washed with PBS, incubated in 100 mM glycine in PBS to quench unreacted biotin, and washed three times with PBS. The cells were then scraped from the dish and pelleted by centrifugation in a clinical centrifuge for 3–5 min. The cell pellet was suspended in lysis buffer (150 mM NaCl, 5 mM EDTA, 50 mM HEPES pH 7.4, 1% Triton X-100, 0.5% protease inhibitor cocktail III (Calbiochem), and 10 μM PMSF) and incubated 30 min. 250 μl of lysis buffer was used for each 100-mm dish of cells (<0.5 mg protein). The extract was clarified by centrifugation at 10,000 *g* for 15 min.

For immunoprecipitation, 200 μl of extract was first incubated for 1 h with 50 μl protein A beads to remove proteins that bound nonspecifically to the protein A. The beads were removed by centrifugation. 15 μl of A7116 or B4947 antibody (see below) was added to the extract and the extract was incubated overnight. The antigen–antibody complex was recovered by incubating with 50 μl of protein A beads for 2 h. The beads were collected by centrifugation at 10,000 *g* for 10 min and then washed four times with 1 ml lysis buffer containing 250 mM NaCl before eluting the bound proteins with Laemmli SDS buffer.

Another aliquot of the extract was used for separating biotinylated from total proteins. 200 μl of extract was incubated with 100 μl of streptavidin beads (Pierce Chemical Co.) overnight with gentle agitation. The beads were collected by centrifugation at 10,000 *g* for 10 min. The beads were washed four times with 0.6 ml lysis buffer + 200 mM NaCl. The bound biotinylated proteins were eluted with 200 μl 2× Laemmli buffer.

Protein samples were run on 4–15% gradient polyacrylamide gels in 25 mM Tris-HCl, pH 8.3, 200 mM glycine, 0.5% SDS with ~10 μg of protein per well. The proteins were electrophoretically transferred to Hybond nitrocelluose membranes in 25 mM Tris-HCl, pH 8.3, 200 mM glycine, 20% methanol. The membranes were blocked with 5% dry milk in PBS with 0.1% Tween-20 (PBS-T) overnight at 4°C or 1 h at room temperature. Depending on the experiment, the nitrocellulose was probed with (a) primary antibody (1/1,000 dilution) followed by horseradish peroxidase–conjugated goat anti–rabbit IgG (1/7,000) (Jackson ImmunoResearch Laboratories) in PBS-T with 1% dry milk or (b) horseradish peroxidase–conjugated streptavidin (Pierce Chemical Co.). Immunoreactive or streptavidin-reactive bands were visualized by enhanced chemiluminescence (ECL kit; Amersham Biosciences).

Two different antibodies were used in this study. Antibodies were raised in rabbits to KLH-conjugated peptides. Antibody B4947 was raised against the 15 COOH-terminal residues of mBest2 (^{494}PWLPSPIGEEEESPA^{508}). This antibody recognizes mBest2 and hBest2 specifically. Antibody A7116 was raised against a domain that is highly conserved in all bestrophins (^{309}LINPFGEDDDDFETN^{323}). This antibody recognizes all the bestrophins we have examined.

RESULTS

mBest2 Behaves as a Ca^{2+}-dependent Cl^- Channel in HEK-293 Cells

mBest2 was expressed in HEK-293 cells by transient transfection. Cells were subjected to whole-cell patch-clamp using solutions that either eliminated cation currents or set the Nernst potentials of cation currents and Cl^- currents at very different values (see MATERIALS AND METHODS). Free Ca^{2+} was buffered to different levels with EGTA. In HEK-293 cells transfected with GFP alone, currents were consistently small regardless of the intracellular free $[Ca^{2+}]$ (Fig. 1). Currents at +100 mV were 4.9 ± 0.9 pA/pF (n = 11) with <20 nM free Ca^{2+} and 6.6 ± 2.3 pA/pF (n = 10) with free $[Ca^{2+}]$ >600 nM. In contrast, cells transfected with GFP and mBest2 exhibited a Ca^{2+}-stimulated Cl^- current. With intracellular free $[Ca^{2+}]$ <20 nM, the currents in mBest2-

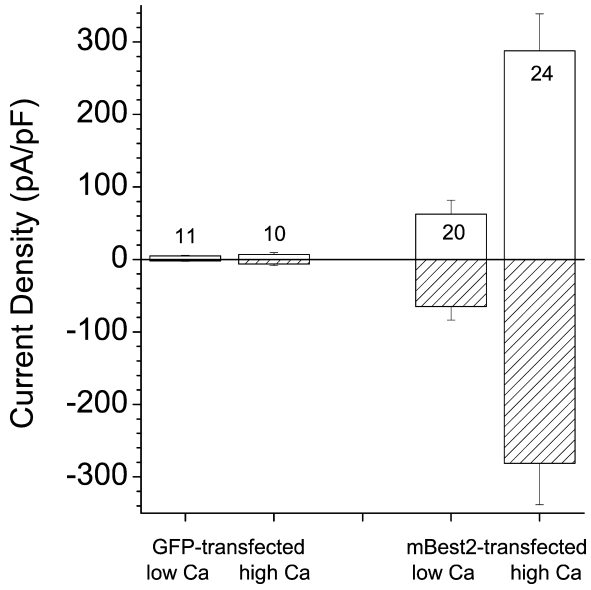

FIGURE 1. Mean current amplitudes in mBest2-expressing HEK-293 cells. HEK-293 cells were transfected with either EGFP alone (GFP-transfected) or mBest2 with EGFP (mBest2-transfected) as described in MATERIALS AND METHODS. Whole-cell voltage clamp recording was performed 1–3 d after transfection. The membrane potential was stepped to different potentials from a 0 mV holding potential for 750 ms. The amplitude of the steady-state currents at the end of the −100 mV (hatched bars, inward currents) and +100 mV (open bars, outward currents) steps were normalized to cell membrane capacitance and expressed as current density. The cells were whole-cell voltage-clamped with pipette solutions containing either <20 nM free Ca^{2+} (low Ca^{2+}) or Ca^{2+} concentrations between 0.6 μM and 4.5 μM (high Ca^{2+}). As shown in Fig. 2, the effect of Ca^{2+} is constant between 0.6 and 4.5 μM. The bars show the means ± SEM of the number of cells indicated within or above the bars.

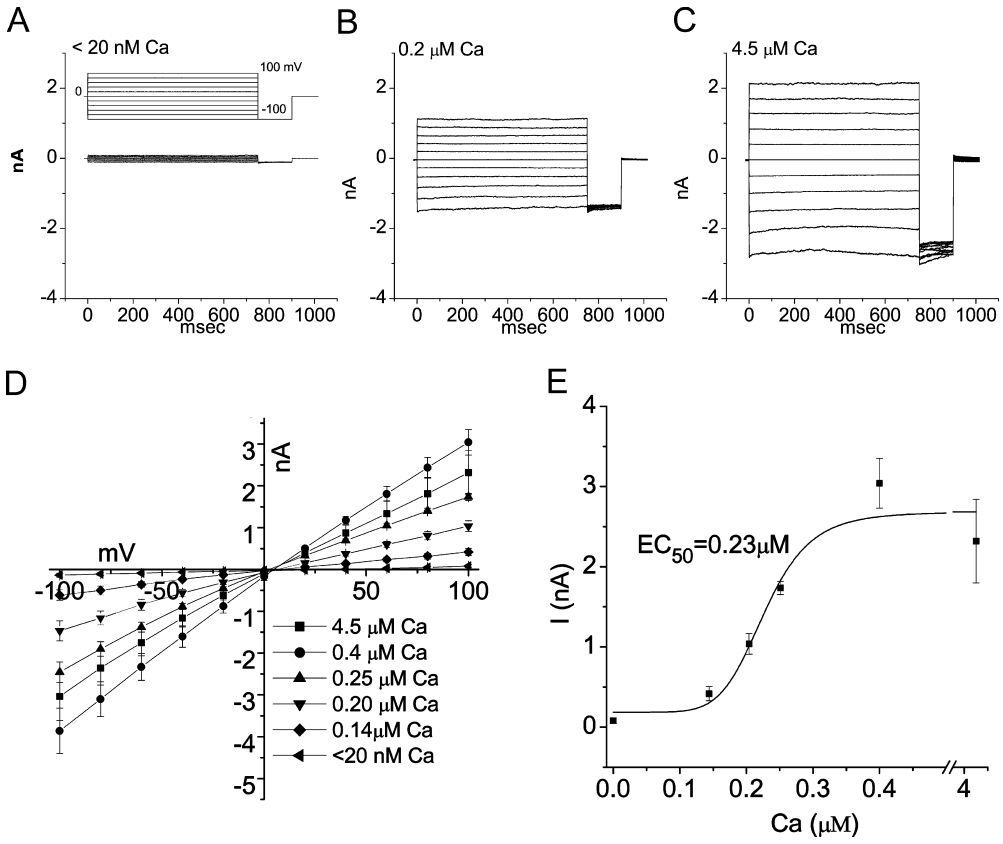

FIGURE 2. Sensitivity of mBest2 currents in HEK-293 cells to intracellular [Ca^{2+}]. HEK-293 cells cotransfected with mBest2 and EGFP were whole-cell voltage-clamped with pipette solutions containing various free [Ca^{2+}]. The voltage clamp protocol is shown above A. (A) Current traces with <20 nM free Ca^{2+}. The current density was <30 pA/pF at +100 mV, which was typical of 13/20 cells studied. (B) Current traces with 0.2 μM free intracellular Ca^{2+}. (C) Current traces with 4.5 μM free intracellular Ca^{2+}. (D) Mean current-voltage relationships obtained from cells with intracellular free Ca^{2+} concentrations of <20 nM (left triangles), 0.14 μM (diamonds), 0.20 μM (down triangles), 0.25 μM (up triangles), 0.40 μM (circles), and 4.5 μM (squares). (E) Dependence of the current on intracellular [Ca^{2+}]. The amplitude of the average currents at +100 mV (squares) was plotted versus [Ca^{2+}] and fitted to the Hill equation (solid line). $n = 7$ in D and E for each [Ca^{2+}].

expressing cells averaged 62.5 ± 19.4 pA/pF ($n = 20$). This was significantly larger than in GFP-transfected cells. When free [Ca^{2+}] was raised to >600 nM, the currents were 4.6-fold larger (287 ± 51.4 pA/pF, $n = 24$).

Current traces of mBest-2 transfected HEK-293 cells are shown in Fig. 2, A–C. The currents were very small when intracellular-free Ca^{2+} was <20 nM (Fig. 2 A). The currents increased with higher [Ca^{2+}] (Fig. 2, B and C). The Ca^{2+}-activated currents were time and voltage independent and exhibited little or no rectification. The I-V relationships were linear for all [Ca^{2+}] and reversed near 0 mV as expected for a Cl^- selective current (Fig. 2 D). A plot of mean current amplitudes versus [Ca^{2+}] showed that the EC_{50} for Ca^{2+} was 230 nM (Fig. 2 E). These currents were mediated by anion-selective channels, as shown by several criteria discussed below.

Ionic Selectivity

The measured reversal potential of the current (E_{rev} = −2.1 ± 0.9 mV, $n = 16$) agreed with the calculated Nernst equilibrium potential for Cl^- (0 mV with 150 mM Cl^- on both sides of the membrane). In most experiments, the major intracellular cation was Cs^+ and the major extracellular cation was Na^+. Thus, if the channel were selectively permeable to Cs^+ or Na^+, the reversal potential would differ significantly from 0 mV. Replacement of extracellular monovalent cations with $NMDG^+$ had no significant effect on bestrophin conductance (G_{Cl} in $NMDG^+$ was 0.91 ± 0.05, $n = 5$, of G_{Cl} in Na^+). The current exhibited an anionic permeability order of $SCN^- > I^- > Br^- > Cl^- > F^-$ (Fig. 3). The relative permeabilities were measured by the shift in reversal potential of the current under bi-ionic conditions. The permeability ratios relative to Cl^- (P_X/P_{Cl}) were 8.2 ± 1.3 for SCN^-, 1.9 ± 0.1 for I^-, 1.4 ± 0.1 for Br^-, and 0.5 ± 0.1 for F^- (n = 8–13). Aspartate was relatively impermeant, but this was not quantified.

Expression in Other Cell Lines

The fact that HEK-293 cells expressing mBest2 have a Ca^{2+}-activated Cl^- current that is absent in nontransfected cells suggests, but does not prove, that these currents are carried by mBest2. Another possibility is that mBest2 expression up-regulates an endogenous cur-

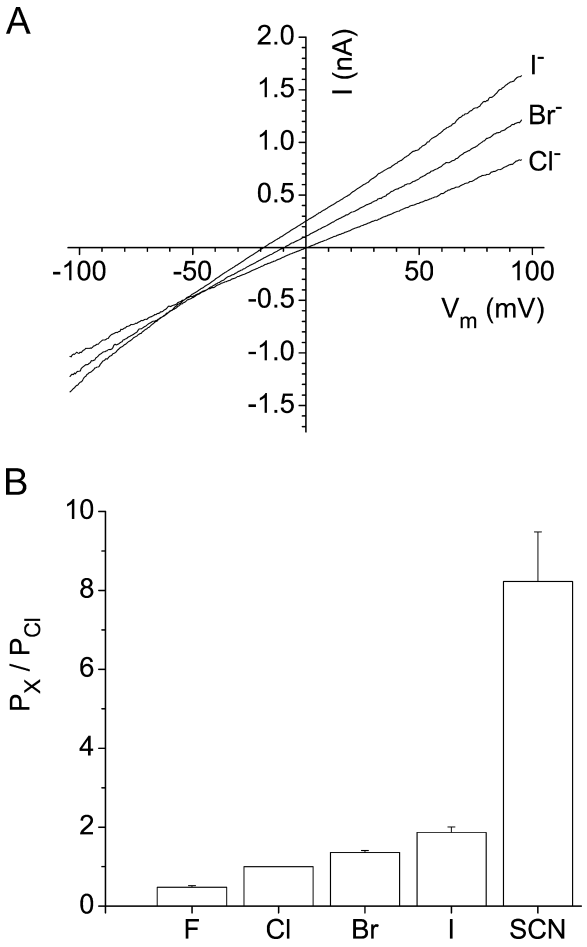

FIGURE 3. Ionic selectivity of the currents in mBest2-transfected HEK-293 cells. HEK-293 cells expressing mBest2 were voltage clamped with 4.5 μM intracellular free Ca^{2+}. (A) Typical current-voltage relationship from one of five experiments showing the relative shift in E_{rev} with I^-, Cl^-, and Br^-. The current-voltage relationships were obtained with a ramp voltage protocol from −100 to +100 mV with 140 mM extracellular Cl^-, Br^-, or I^- as indicated. (B) Relative permeability ratios (P_X/P_{Cl}) of mBest2. P_X/P_{Cl} was calculated from the Goldman-Hodgkin-Katz equation. The permeabilities of SCN^- and F^- relative to Cl^- were performed in a separate set of experiments than those for I^- and Br^-. See Fig. 6 A for the current-voltage relationship for SCN^-.

rent or alters the trafficking of an endogenous channel to the plasma membrane.

To test whether the current might be due to up-regulation of an endogenous current, mBest2 was expressed in several different cell lines. We assumed that if the properties of the current were the same in different cell lines, this would strengthen the likelihood that the current was encoded by mBest2. Expression of mBest2 in HeLa cells (Fig. 4, A–C) and in ARPE-19, a human retinal epithelial cell line (Fig. 4 D), produced Ca^{2+}-activated Cl^- currents that were similar to the one in HEK-293 cells. GFP-transfected HeLa cells had very small Cl^- currents in both low and high Ca^{2+}. When HeLa cells were transfected with mBest2, Ca^{2+}-activated Cl^- currents appeared. The amplitudes of these currents were similar, or perhaps slightly smaller than those in HEK-293 cells. Untransfected ARPE-19 cells exhibited a small endogenous Ca^{2+}-activated Cl^- current that was strongly outwardly rectifying. Transfection with mBest2 induced a Ca^{2+}-activated Cl^- current that differed from the endogenous current in that the induced current had a linear I-V relationship. The induced currents in ARPE-19 cells were significantly smaller than those we observed in HEK-293 cells.

Bestrophin Localization on the Plasma Membrane

If mBest2 carries the current, it should be expressed on the cell surface. To test this, we determined whether bestrophin was labeled by membrane-impermeant biotinylation reagents in intact cells. Intact cells were labeled at 4°C with NHS-LC-Biotin and the cells were lysed in a buffer containing Triton X-100. mBest2 was then immunoprecipitated using an antibestrophin antibody (A7116). The immunoprecipitate was run on SDS-PAGE, transferred to nitrocellulose, and probed using HRP-labeled streptavidin (Fig. 5, lane 1). A 64-kD band that corresponded to mBest2 was observed. Non-transfected HEK cells yielded no band (lane 2). These data provide evidence that mBest2, at least under conditions of heterologous expression, is located at the cell surface. To be certain that the biotinylation reaction did not label intracellular proteins, biotinylated proteins were recovered from an aliquot of the lysate using steptavidin beads. The total extract and the proteins eluted from the streptavidin beads were run on an SDS-gel, transferred to nitrocellulose, and blotted with an antibody against actin. A 46-kD band was labeled in total extract (lane 3), but no band was observed in the fraction eluted from the streptavidin beads (lane 4). Thus, intracellular proteins were not labeled by the biotinylation reaction. The fraction that bound to the streptavidin beads, however, contained mBest2 because a 64-kD band was observed when this fraction was probed with anti-mBest2 antibody (B4947) (lane 5). The finding that bestrophin was present on the cell surface excluded the possibility that bestrophin caused up-regulation of an endogenous channel without itself being incorporated into the plasma membrane.

Mutagenesis

To test further the hypothesis that mBest2 was responsible for carrying the Ca^{2+}-activated Cl^- current observed in mBest2-expressing cells, we performed site-directed mutagenesis on mBest2. The objective was to find a mutation that altered the ionic permeability or conductance of the channel. Such a mutation would provide evidence that mBest2 either contained the selectivity filter or controlled channel gating. We focused on a region of

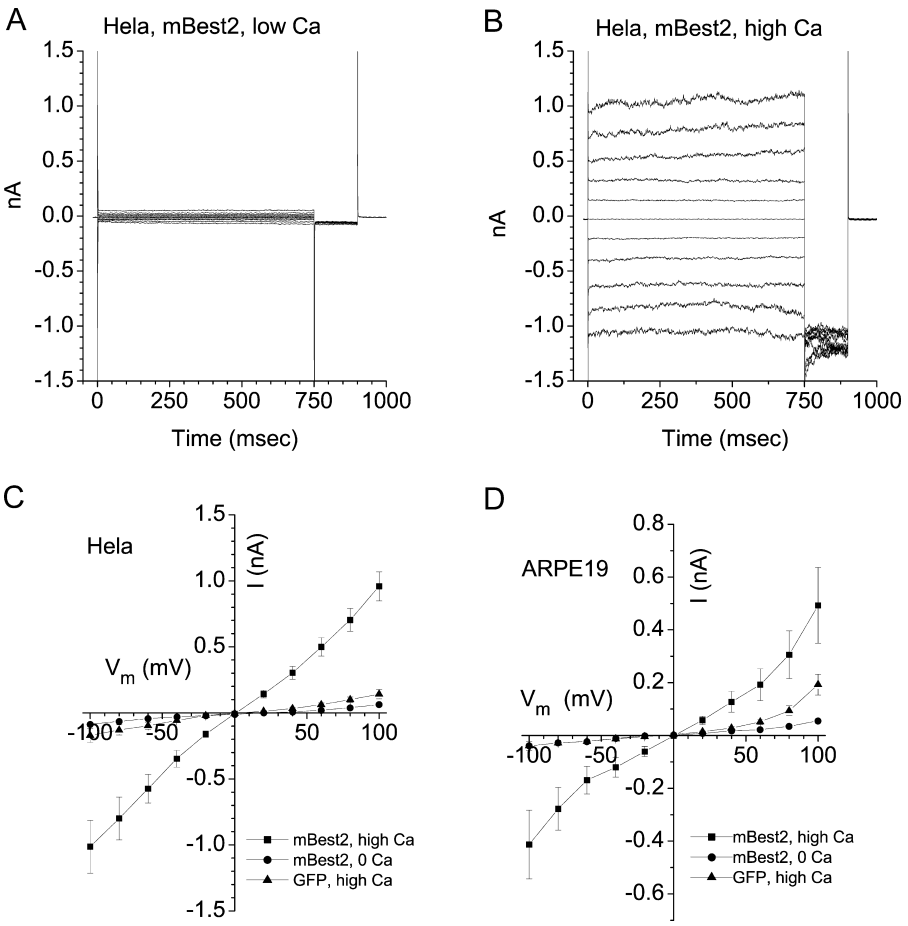

FIGURE 4. mBest2 currents in HeLa and ARPE-19 cells. Whole-cell recording was done as in Fig. 2. (A) Current traces of a HeLa cell with <20 nM free Ca^{2+} in pipette. (B) Current traces of a HeLa cell with 4.5 μM Ca^{2+} in pipet. (C) Current-voltage relationships of mBest2 currents in HeLa cells. The steady-state currents at the end of the voltage steps were plotted against V_m for cells transfected with EGFP alone and recorded with 4.5 μM Ca^{2+} in the pipet (n = 7, triangles), for mBest2 transfected cells recorded with <20 nM Ca^{2+} in the pipette (n = 6, circles), and for mBest2 transfected cells with 4.5 μM Ca^{2+} in the pipet (n = 8, squares). (D) Current-voltage relationships of mBest2 currents in ARPE-19 cells. Cells were transfected with EGFP alone and recorded with 4.5 μM Ca^{2+} in the pipet (n = 6, triangles), or transfected with mBest2 and recorded with <20 nM pipet Ca^{2+} (n = 4, circles) or 4.5 μM pipet Ca^{2+} (n = 6, squares).

the protein that was homologous to a region in hBest1 suggested by Tsunenari et al. (2003) to be important in channel function. We find that mutations in S79 produce changes in ionic conductance that are consistent with this residue playing an important role in anion binding (Fig. 6). In wild-type channels, substitution of extracellular Cl^- with SCN^- produced a significant decrease in conductance and a shift of the E_{rev} −47.8 ± 3.8 mV (Fig. 6 A, n = 13). This suggested that SCN^- was more permeant than Cl^- (SCN^- entered the channel more easily than Cl^-), but that SCN^- was less conductive than Cl^- (SCN^- bound in the pore more tightly than Cl^-). With the S79C mutant, in contrast, substitution of SCN^- for Cl^- did not reduce the conductance and shifted the E_{rev} only −31.7 ± 2.2 mV (Fig. 6 B, n = 10). The smaller shift in E_{rev} in S79C compared with wild-type channels showed that relative SCN^- permeability was reduced by the mutation. P_{SCN}/P_{Cl} was 8.2 ± 1.3 for wild-type and 3.9 ± 0.4 for S79C channels ($P < 0.01$, Fig. 6 C). The difference in the relative SCN^- conductance (G_{SCN}/G_{Cl}, measured as slope conductance at +50 mV driving force) through S79C and wild-type channels was very large. In wild-type channels, G_{SCN}/G_{Cl} = 0.14 ± 0.03 (n = 8), whereas for the S79C mutant the ratio was 0.96 ± 0.04 (n = 6) ($P < 0.01$, Fig. 7 A). The conductance in both the inward and outward directions was reduced by extracellular SCN^- (Fig. 7 A). This suggests that not only is SCN^- less conductive than Cl^-, it is also able to block outward movement of Cl^- (inward current), presumably by binding in the channel pore.

To gain additional insight into the mechanisms of SCN^- interaction with wild-type and S79C mutant channels, we examined the effects of intracellular SCN^- on the currents. Cells were whole-cell voltage clamped with an SCN^- containing intracellular solution and the extracellular solution was switched between SCN^- and Cl^-. In wild-type channels, both inward and outward currents were significantly smaller with SCN^-_{in} than with Cl^-_{in} (Fig. 7 B, hatched bars) This suggests that SCN^- was able to block the current from the inside as well as from the outside. Switching from extracellular Cl^- to SCN^- had little additional effect on conductance in either the inward or outward direction (Fig. 7 A). S79C currents recorded with symmetrical Cl^- were smaller than wild-type currents (Fig. 7 B, open bars). The amplitudes of the currents were not affected by either internal or external SCN^- (Fig. 7, A and B, open bars). These data suggest that SCN^- binds to a site within the pore more tightly than Cl^-

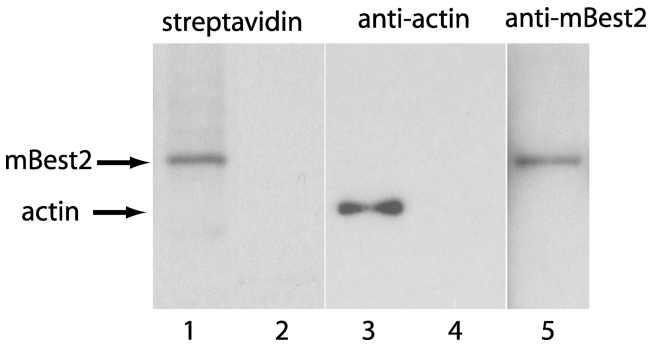

FIGURE 5. Localization of mBest2 in the plasma membrane of HEK-293 cells. Lanes 1 and 2: streptavidin labeling of immunoprecipitated proteins. Nontransfected (lane 2) or mBest2-transfected (lane 1) HEK-293 cells were labeled with membrane-impermeant NHS-LC-biotin and lysed. mBest2 was immunoprecipitated with A7116 antibody, run on SDS-PAGE, and transferred to nitrocellulose. The nitrocellulose was then probed with HRP-conjugated streptavidin. A 64kD band was observed in transfected, but not nontransfected cells. Lanes 3–5: Western blots. Lane 3: total extract from mBest2-transfected cells was probed with antibody to α-actin. Lanes 4 and 5: the extract from mBest2-transfected cells was incubated with streptavidin-beads to collect biotinylated proteins. Biotinylated proteins were then probed with antibody to α-actin (Lane 4) or B4947 mBest2-specific antibody (Lane 5).

and that the S79C mutation reduces the affinity of this site for SCN^-.

SCN^- Block of Cl^- Currents

To test the hypothesis that serine-79 is involved in anion binding in the pore of the mBest2 channel, we examined the ability of extracellular SCN^- to block Cl^- currents in wild-type and S79C mutants. In accordance with our expectation, SCN^- blocked wild-type Cl^- conductance with an apparent affinity of ~12 mM (Fig. 8, A, C, and E). However, SCN^- had no significant blocking effect on S79C currents (Fig. 8, B, D, and E). These data show that SCN^- had a much higher affinity in the pore of wild-type channels than it did in the pore of S79C channels.

Sulfhydryl Modification of S79C

Cysteine mutagenesis has been a very powerful tool for probing the structure of ion channels (Akabas et al., 1992; Karlin and Akabas, 1998). By mutating residues in the channel to cysteines and then examining the effect of sulfhydryl reactive reagents that do not cross the membrane, it has been possible to deduce the sidedness and accessibility of different residues and to evaluate the role of charge in ion permeation. To determine whether the binding and permeation of anions might be affected by electrostatic charge around serine-79, we examined the effects of charged sulfhydryl reagents on the properties of the current associated with the S79C mutant. In cells transfected with wild-type mBest2, 1 mM $MTSET^+$, 100 μM $MTSES^-$, or 100 μM MTSEA applied to the bath produced no effect or only a small stimulation of the current (Fig. 9, A and D). In contrast, with S79C currents, 10 μM $MTSET^+$ produced an average ~6-fold increase in current amplitude within 30 s (Fig. 9, B and D). The increase in the current was abolished by preincubating $MTSET^+$ with an excess of reducing agent (DTT or β-mercaptoethanol; not depicted). The effect of $MTSET^+$ was reversed by 5 mM DTT (Fig. 9 B). The current was also stimulated irreversibly by N-ethyl maleimide (not depicted). These data provide strong evidence that the stimulation of the current was due to modification of a sulfhydryl residue in mBest2. To test whether the effect of $MTSET^+$ was mediated by the cysteine introduced at position 79 or was due to a conformational change that made an endogenous cysteine accessible to $MTSET^+$, we examined the effect of $MTSET^+$ on S79A and S79L mutations. Currents induced by these mutations were not stimulated by 10 μM $MTSET^+$ (Fig. 9 D). The apparent decrease in the S79A current produced by $MTSET^+$ was actually due to an uncorrected time-dependent rundown in this current. These data show that the effect of $MTSET^+$ required the cysteine at position 79 and was not caused by a conformational change in the protein revealing an endogenous cysteine.

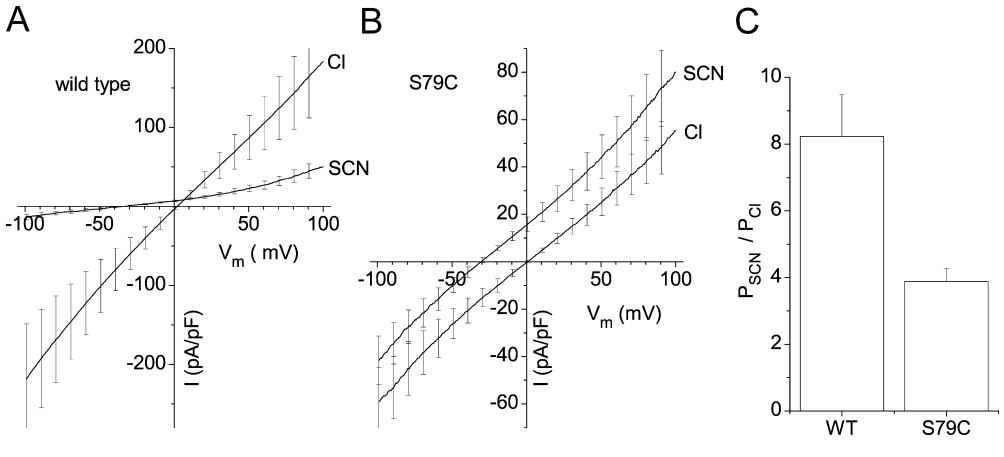

FIGURE 6. SCN^- conductance in wild-type and S79C mutant mBest2. Current voltage relationships were determined by voltage ramps with 4.5 μM intracellular Ca^{2+}. HEK-293 cells were transfected with wild-type (A) and S79C mutant (B) of mBest2, respectively. Bathing solution was either normal Cl^- containing solution or one in which 140 mM Cl^- was replaced with SCN^- as indicated. (C) Mean P_{SCN}/P_{Cl} ratios for wild-type (n = 8) and S79C (n = 6).

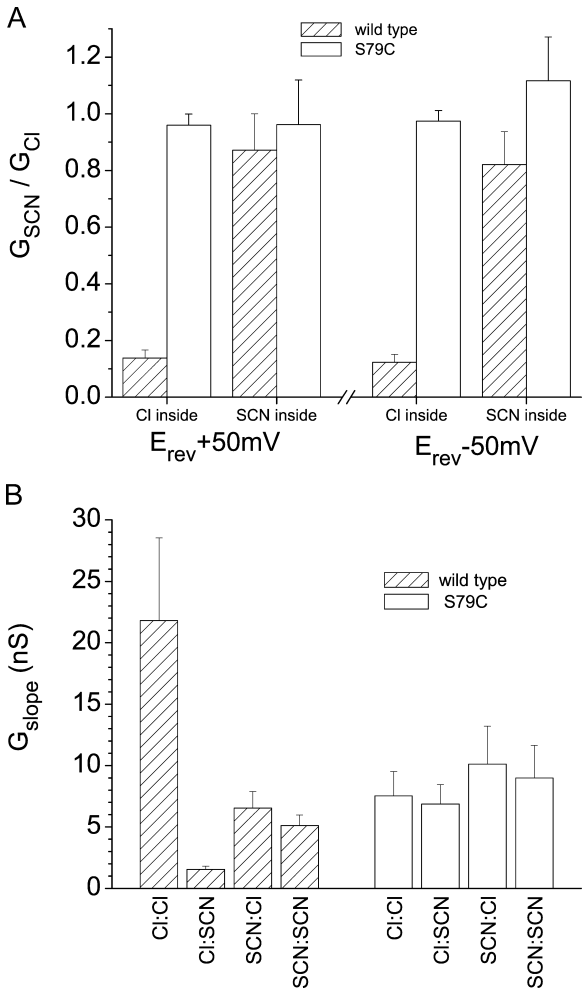

FIGURE 7. Relative conductances of Cl^- and SCN^- in wild-type and S79C mutant mBest2. Experiments were performed essentially as shown in Fig. 6. (A) Ratio of conductance with SCN^- outside to conductance with Cl^- outside is plotted for intracellular Cl^- or intracellular SCN^- for wild-type (hatched bars) and S79C (open bars) currents. Conductance was measured as the slope of the current-voltage relationship between E_{rev} and E_{rev} +50 mV (left side) or E_{rev} −50 mV (right side). (B) Mean slope conductance (measured between E_{rev} and E_{rev} +50 mV) is plotted for wild-type mBest2 (hatched bars) and S79C mBest2 (S79C, open bars) for different combinations of intracellular and extracellular (in:out) Cl^- and SCN^- shown on the x-axis.

The increase in current amplitude produced by $MTSET^+$ in the S79C mutant was due to an increase in conductance with no apparent change in ionic selectivity (Fig. 9 E). $MTSET^+$ increased the current carried by either Cl^- or SCN^-, but it did not change the selectivity for either anion, because the E_{rev} was the same before and after $MTSET^+$ application (Fig. 9, D and E). Thus, although $MTSET^+$ significantly altered the conductance, it had no apparent effect on the relative anionic permeability. $MTSES^-$ (10–100 μM) (Fig. 9, B and D) also stimulated the current, but the effect was smaller and slower than the effect produced by the same concentration of $MTSET^+$ (Fig. 9 B). These data show that modification of serine-79 affected conductance, but they suggest that charge is not important at this residue because $MTSET^+$ and $MTSES^-$ have similar effects, as does NEM, which is uncharged.

Pharmacology of S79C Mutations

The S79C currents, in addition to differing from wild-type currents in relative conductance, also differed quantitatively from wild-type currents in their pharmacology (Fig. 10). Wild-type currents were blocked by DIDS with an IC_{50} of 3.1 ± 0.3 μM. The S79C currents were approximately fivefold less sensitive to DIDS than wild-type currents with an IC_{50} = 14.6 ± 3.6 μM for S79C. Block of the currents by DIDS was not significantly voltage-dependent.

DISCUSSION

Heterologous Expression to Identify Cl^- Channel Genes

The use of heterologous expression is a powerful technique for identifying the type of channel encoded by a cloned gene. This technique is not without limitations, however. Expressed channels can have properties different than native channels because of missing subunits. For example, the behavior of an ion channel is often dependent on the composition of the various subunits that come together to form the pore of a heteromeric channel. The effect of subunit composition is clearly demonstrated in G-protein gated K channels where the channel is virtually nonfunctional unless it is composed of the correct mixture of different pore-forming subunits (Dascal, 1997; Isomoto et al., 1997). In addition, auxiliary cytoplasmic subunits are also important in channel function. In voltage-gated Ca^{2+} channels, the function of the pore-forming α_1 subunit is dramatically altered by auxiliary β and α_2-δ subunits (Arikkath and Campbell, 2003). Another complication of heterologous expression is the presence of endogenous channels or subunits whose expression or trafficking can be altered by expression of a heterologous protein. This has been clearly observed in *Xenopus* oocytes, where expression of a variety of membrane proteins results in up-regulation of an endogenous current (see Kuruma et al., 2000 for references and discussion).

These limitations provide an obstacle to identification of new Cl^- channel genes in particular, because probably every cell expresses Cl^- channels of various types and it is difficult to find cell types that are naïve recipients of new Cl^- channels. Furthermore, unlike cation channels, the pharmacology of Cl^- channels remains sufficiently unrefined that it is often not possible to unambiguously identify a Cl^- channel on the basis of its pharmacology. For example, it is a contentious issue

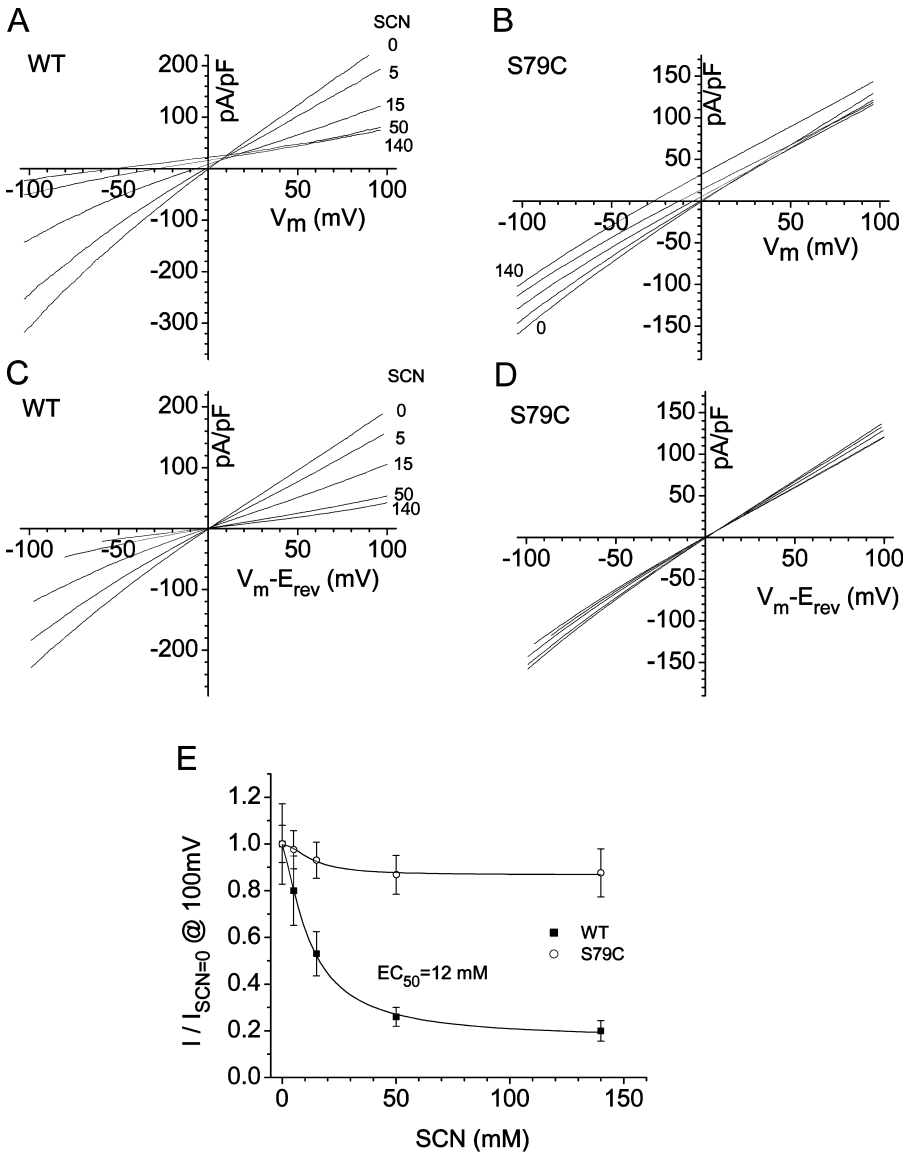

FIGURE 8. Dose-dependent block of mBest2-expressed currents by extracellular SCN^-. The experiments were performed as in Fig. 8. (A and B) I-V relationships of wild-type– (A) or S79C (B) mBest2-expressing HEK-293 cells with different extracellular solutions in which varying amounts of Cl^- (5–140 mM) were replaced with equimolar amounts of [SCN^-] as indicated. (C and D) The currents in A and B were replotted versus driving force (V_m-E_{rev}) for each anion mixture. (E) Dose-dependent block by SCN^-. The relative current at +100 mV in C and D for each anion mixture was plotted as a function of [SCN^-] for wild-type (filled squares, $n = 5$) and the S79C mutation (open circles, $n = 6$).

whether CLCA proteins are Ca^{2+}-activated Cl^- channels. Expression of members of the CLCA family in mammalian cells has been reported to induce Ca^{2+}-activated Cl^- currents (Ji et al., 1998; Fuller and Benos, 2000; Elble et al., 2002), but other investigators believe that there is insufficient evidence to establish CLCAs as Ca^{2+}-activated Cl^- channels (Jentsch et al., 2002). The endogenous expression of CLCA transcripts does not correlate with Ca^{2+}-activated Cl^- currents (Papassotiriou et al., 2001) and the Ca^{2+} sensitivity of these channels is much higher than endogenous Ca^{2+}-activated Cl^- channels. Others have suggested that CLCAs are Cl^- channel regulators (Loewen et al., 2002a,b). Another controversial family of putative Cl^- channel includes the p64 and CLIC proteins. These proteins have failed to gain acceptance as Cl^- channels not only because they exist in both transmembrane and cytosolic soluble forms, but also because, like the CLCAs, mutagenesis and knock-out evidence for their function as a channel is limited.

Evidence that Bestrophins Are Cl^- Channels

There is now growing evidence that bestrophins are a new family of Cl^- channels, but it is important to avoid the same ambiguity that surrounds the CLCAs and CLICs. Bestrophins from human, *Drosophila*, *C. elegans*, and *Xenopus* have now been expressed heterologously by two laboratories with similar results (Sun et al., 2002; Qu and Hartzell, 2003; Tsunenari et al., 2003). The fact that different bestrophins exhibit different waveforms and rectification properties is reassuring: it suggests that they are indeed Cl^- channels or interesting regulators of Cl^- channels. The fact that hBest1 is expressed as a Cl^- channel also fits well with the explanation that

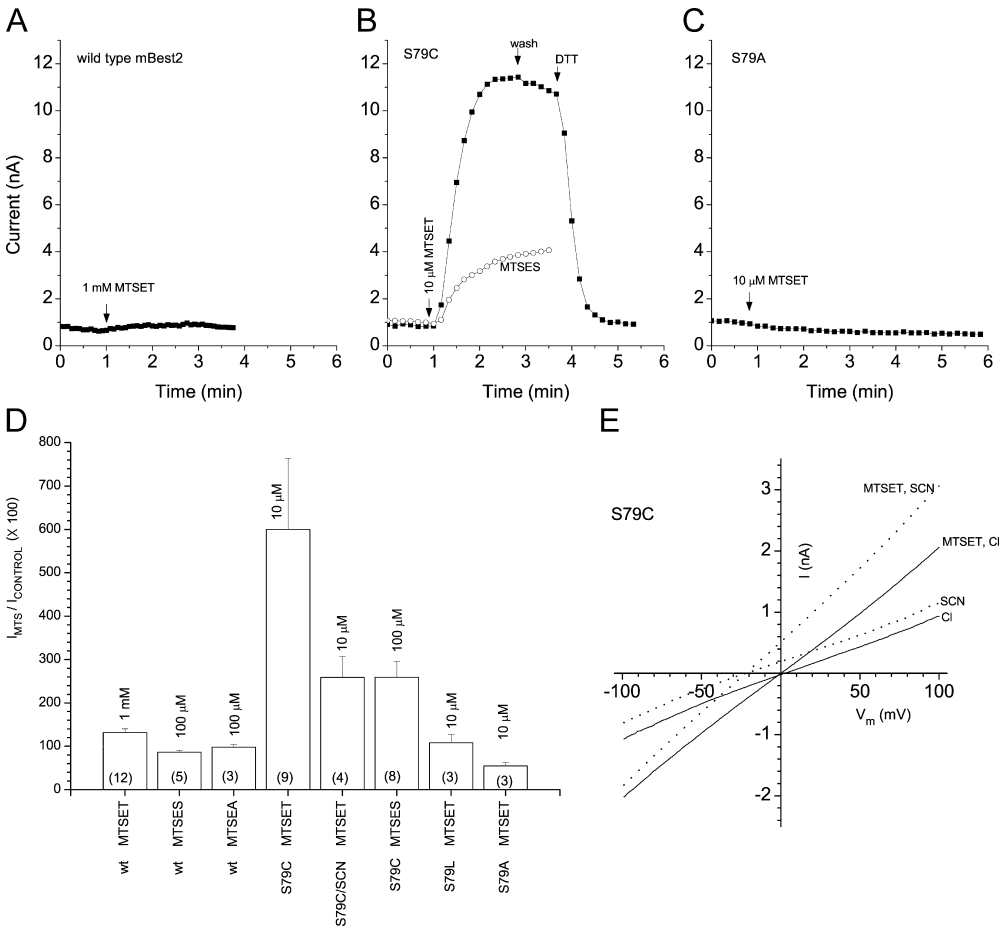

FIGURE 9. Effect of sulfhydryl reagents on wild-type and S79 mutant mBest2. Currents were recorded using a high intracellular free [Ca^{2+}]. (A–C) Time course of the effect of MTS reagents on mBest2 currents at 100 mV. (A) Effect of 1 mM $MTSET^+$ on currents induced by wild-type mBest2. (B) Effect of 10 μM $MTSET^+$ (solid symbols) and 10 μM $MTSES^-$ (open symbols) on currents induced by S79C mBest2. (C) Effect of 10 μM $MTSET^+$ on currents induced by S79A mBest2. Note the rundown of the S79A current during the first 2 min of recording. (D) Mean effect of MTS reagents on wild-type (wt) and S79C, S79A, and S79L mBest2 currents. The ratio of the control current at +100 mV before application of the MTS reagent ($I_{control}$) and after the effect reached steady-state (I_{MTS}) is shown. The concentration of reagent used is shown above each bar and the number of cells tested is shown within the bar. Symmetrical Cl^- was used for all experiments except the experiment labeled S79C/SCN MTSET, where 140 mM Cl^- was replaced with SCN^-. (E) Current-voltage relationships of S79C currents before and after $MTSET^+$ in the presence of symmetrical Cl^- (solid lines) and with extracellular Cl^- replaced with SCN^- (dashed lines) as indicated.

Best vitelliform macular dystrophy is caused by a functional defect in a basolateral Cl^- channel in the retinal pigment epithelium (Sun et al., 2002).

Here, we show that transfection of three types of cells with mBest2 results in expression of a Ca^{2+}-stimulated Cl^- current. Although the current is stimulated by Ca^{2+}, it apparently is not absolutely dependent on Ca^{2+}, because mBest2-transfected cells have elevated currents even with intracellular solutions containing <20 nM free Ca^{2+}. Whether this is a consequence of overexpression or whether the channels have a finite opening probability in the absence of Ca^{2+} remains to be seen. In any case, as we reported for *Xenopus* Best2 (Qu and Hartzell, 2003), the waveform and rectification of these currents are different than those of endogenous Ca^{2+}-activated Cl^- currents in *Xenopus* oocytes. The bestrophin currents are time independent and exhibit little rectification at any Ca^{2+} concentration, whereas "classical" *Xenopus* oocyte Ca^{2+}-activated Cl^- currents outwardly rectify and exhibit voltage-dependent kinetic activation and deactivation at low and moderate Ca^{2+} concentrations (Kuruma and Hartzell, 2000; Machaca et al., 2002). Furthermore, block of mBest2 by DIDS is voltage-independent, whereas "classical" Ca^{2+}-activated Cl^- channels are blocked in a voltage-dependent manner by DIDS (Qu and Hartzell, 2001). Thus, it seems unlikely that bestrophins are responsible for the classical Ca^{2+}-activated Cl^- currents, unless a missing subunit is found that changes these properties.

Bestrophins Are Expressed on Cell Surface, but May Also Function Intracellularly

In our previous study, we presented immunocytochemical evidence that *Xenopus* Best2 is expressed on the cell surface in transfected HEK-293 cells (Qu and Hartzell, 2003). In this paper, we used cell-surface biotinylation to measure cell-surface expression of mBest2. The biotinylation experiments confirm the presence of mBest2 on the surface of transfected cells. However, a considerable fraction of mBest2 is not biotinylated and may therefore be located on intracellular membranes. Con-

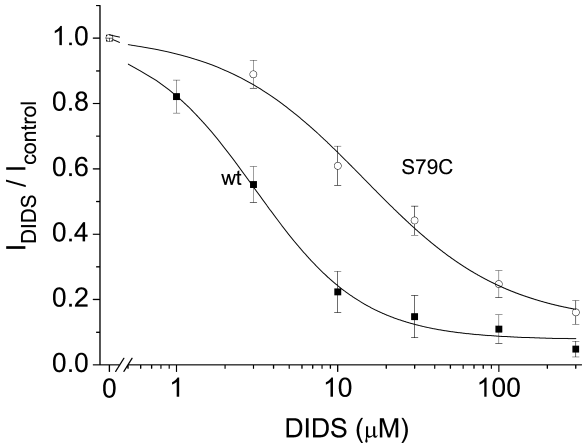

FIGURE 10. Sensitivity of wild-type and S79C mBest2 currents to DIDS. Whole-cell voltage-clamp recordings were performed on mBest2-transfected HEK-293 cells. Blockers were applied to the bathing solutions. The amplitude of the currents at +100 mV in the presence of DIDS relative to currents in the absence of DIDS were plotted for wild-type mBest2 (wt, solid symbols, $n = 4$–6) and for S79C (open symbols, $n = 7$). The data were fit to the Hill equation (solid line).

focal microscopy of immunostained, transfected HEK-293 cells also shows intracellular localization of mBest2. This suggests the possibility that although mBest2 is trafficked to the plasma membrane, at least under conditions of overexpression, mBest2 may also have functions in intracellular membranes. The ClC family of Cl^- channels have recently been shown to play key roles in vesicular trafficking in the endosomal pathway (see references and discussion in Jentsch et al., 2002; Faundez and Hartzell, 2004). ClC channels are important in vesicular function by regulating the intralumenal pH of the vesicle by providing a counter-ion shunt to dissipate the membrane potential generated by the proton pump. But, in addition, because a variety of proteins are Cl^- sensitive, Cl^- channels may also regulate vesicular function via [Cl^-] (Faundez and Hartzell, 2004). Although ClC channels have dominated the field's interest in intracellular Cl^- channels, there are niches where other Cl^- channels could be important. Whether bestrophin will fill one of these niches remains to be seen.

Mechanisms of Ion Permeation through Bestrophin Channels

The currents that are induced upon expression of mBest2 are anion selective. They have an ionic permeability sequence of $SCN^- > I^- > Br^- > Cl^- > F^-$ and a conductance sequence of $I^- > Br^- > Cl^- > F^- > SCN^-$. The permeability ratios are very similar to those we have published for Ca^{2+}-activated Cl^- channels (Qu and Hartzell, 2000) except that F^- is more permeant through the bestrophin channels.

The permeability of an ion reflects the ease with which the ion enters the channel. The permeability sequence of mBest2 is the same as the Eisenman "weak field strength" lyotropic series (for review see Eisenman and Horn, 1983). The "weak field strength" series suggests that interaction between the permeant ion and the channel is weak and that permeability is related to the ease with which the permeant ion leaves the bulk solution and enters the channel. In the case of the CFTR Cl^- channel and the Ca^{2+}-activated Cl^- channel (Smith et al., 1999; Qu and Hartzell, 2000), which have similar permeability sequences to the mBest2 channels studied in this paper, the ease with which the anion enters the pore is related to its hydration energy: larger anions with lower hydration energies can exchange their bound water with hydrophilic structures in the pore more readily than those with higher hydration energies.

Conductance, on the other hand, reflects the interaction of the permeant ion with the channel. Anions that bind more tightly to the channel are conducted less well. In wild-type mBest2 channels, SCN^- is highly permeant, but poorly conductive. The low conductance of SCN^- implies that it resides longer in the pore during transit through the channel than Cl^- does. This suggestion is supported by the observation that low concentrations of SCN^- block Cl^- currents through the bestrophin channels with an IC_{50} of 12 mM.

We observe that block of current by low concentrations of SCN^- is voltage independent. Although one might expect that block of Cl^- current by SCN^- would be voltage dependent if the anion binding site is within the conduction pathway of the channel, the fact that SCN^- is both a blocking ion and a permeant ion complicates the situation. Because voltage would be expected to influence both the on-rate and off-rate of ion binding, it is difficult to predict how voltage dependence would be manifested on macroscopic currents. With CFTR and Ca^{2+}-activated Cl^- channels, block of Cl^- currents by SCN^- is only very weakly voltage dependent (Mansoura et al., 1998; Qu and Hartzell, 2000; Linsdell, 2001). More pronounced voltage-dependence is observed with the more hydrophobic, less conductive anion $C(CN)_3$ (Qu and Hartzell, 2000). This suggests that the voltage dependence of block by SCN^- is likely to be obscured by the fact that it is conductive as well as a blocker.

Structure-function Analysis of Bestrophin

Mutation of S79 to cysteine produced currents that differed significantly from wild-type currents in their relative conductance and permeability. Compelling evidence that S79 is located in the conduction path of the channel is provided by the finding that P_{SCN}/P_{Cl} is less than half that for wild-type currents and that the S79C

mutation alters the binding of anions in the pore of the channel. S79C currents had relative SCN^- conductances that were the same as, rather than less than Cl^-, and SCN^- was unable to block Cl^- currents in the mutant channels.

Ion binding is the property of ion channels that is most indicative of ion-channel interaction (Mansoura et al., 1998). For example, in the K^+ channel Kv2.1, mutation of a valine to a leucine in the pore loop alters the conductance of Rb^+ relative to K^+ almost 10-fold while changing P_{Rb}/P_K only <50% (Kirsch et al., 1992; Taglialatela et al., 1993). This valine maps to valine-76 in the KcsA channel. In KcsA, the carbonyl oxygen of valine-76 plays a key role in coordinating K^+ ions in the pore (Doyle et al., 1998; Zhou et al., 2001). Similarly, mutation of certain key residues in CFTR (e.g., G314 and K335) have a dramatic effect on anion binding, as measured by the ability to SCN^- to block Cl^- currents, but have little effect on the anionic permeability sequence (Mansoura et al., 1998). These findings are consistent with the interpretation that permeability ratios depend more strongly on ion-water interactions than on channel–ion interactions. Because SCN^- has a low hydration energy, its interaction with the channel is likely to be relatively more important in defining its conduction through the channel than for ions with stronger interactions with water. This may explain the effects of serine-79 mutations were most easily detected using SCN^-.

Electrostatic interactions do not seem to play an important role in anion binding at position 79, because modification of the S79C mutation with positively and negatively charged MTS reagents produced similar results on conduction. Rather, both $MTSES^-$ and $MTSET^+$ increased Cl^- and SCN^- conductance proportionately with no change in their relative permeability. These data suggested that the simple addition of a larger group on the side chain at position-79 caused an increase in conductance, possibly by distorting the structure of the pore. Consistent with this result was the finding that substitution of S79 with leucine or arginine, which have larger side chains than cysteine or serine, produced currents with larger conductances.

In speculating about the role of S79 in anion conduction in mBest2, one is tempted to extract principles learned from the crystal structures of the bacterial ClC and KscA channels (Doyle et al., 1998; Dutzler et al., 2002, 2003). In both these channels, atoms in the backbone of the polypeptide chain play important roles in ion conduction. Specifically, in the cation channel KscA, backbone carbonyl groups coordinate the permeant K^+ ion, whereas in the bacterial ClC channel, backbone amide nitrogen atoms contribute to the Cl^- binding site. Also, in both cases, helix dipoles contribute an electrostatic component to ion binding. With the bacterial ClC channel, serine-107 also acts as a ligand for Cl^-. Serine-107 is located at the end of a helix and the hydrogen bond formed between the serine hydroxyl and the amide nitrogen of isoleucine-109 makes the serine hydroxyl more polar for interaction with the permeant Cl^- anion. One is tempted to think that the mBest2 may work on similar principles. In the ClC channel, there are no full charges involved in the coordination of the permeant anion. The same may be true in mBest2, where there are no basic amino acids in primary structure within 10 amino acids of S79. Although the three-dimensional structure of mBest2 is not yet known, S79 in mBest2 is one residue from a helix-disrupting proline, suggesting the possibility that it may be near the end of a helix, just as serine-107 in the bacterial ClC is two residues from a proline. Clearly, these speculations await a crystal structure of a bestrophin protein for testing.

Alterations in macroscopic conductance produced by SCN^- and by S79 mutations could in principle be caused by changes in single channel conductance or channel gating. Although formally the possibility exists that SCN^- blocks Cl^- conductance allosterically by binding to a different site not located in the pore, this possibility seems unlikely for several reasons. SCN^- at high concentrations clearly does permeate the channel and therefore enters the pore. The smooth progression from block at low SCN^- concentrations to permeation at high SCN^- concentrations is consistent with block and permeation occurring at the same site. The changes in P_{SCN}/P_{Cl} we observe with the S79C mutation are unlikely to be caused by changes in channel gating because SCN^- and Cl^- conductances would be expected to change in parallel with a change in channel open probability. For example, if open probability were increased by the S79C mutation, one would expect that the conductances for Cl^- and SCN^- would both increase relatively the same amount. Instead, we observe that SCN^- conductance increases ~7-times relative to Cl^- conductance in S79C (Fig. 7 A). An exception to this reasoning could occur if gating and permeation were tightly linked, as they are in ClC channels (Dutzler et al., 2003). Such a link would be likely to occur, however, only if the gate were located within the pore, as it is in ClC channels. Also, the effects of SCN^- were rapid in onset and rapidly reversible, consistent with an effect in the permeation pathway.

Conclusion

In conclusion, we present solid data that mBest2 is a bona fide Cl^- channel. Overexpression results in Ca^{2+}-activated Cl^- currents in several cell lines. mBest2 protein is present on the cell surface. Mutations in mBest2 alter the conduction and binding of anions. Although it is known that mutations in hBest1 are associated with

early-onset macular degeneration, the mechanisms underlying this disease remain unknown. Furthermore, the functions of the other three mammalian bestrophins, including mBest2, remain unknown.

The authors thank Chun Pfhanl and Toni Grim for excellent technical assistance.

Supported by NIH grants GM60448 and EY014852. R. Fischmeister also received support from INSERM.

Olaf S. Andersen served as editor.

Submitted: 20 January 2004
Accepted: 2 March 2004

REFERENCES

Akabas, M.H., D.A. Stauffer, M. Xu, and A. Karlin. 1992. Acetylcholine receptor channel structure probed in cysteine-substitution mutants. *Science.* 258:307–310.

Arikkath, J., and K.P. Campbell. 2003. Auxiliary subunits: essential components of the voltage-gated calcium channel complex. *Curr. Opin. Neurobiol.* 13:298–307.

Bakall, B., T. Marknell, S. Ingvast, M.J. Koisti, O. Sandgren, W. Li, A.A. Bergen, S. Andreasson, T. Rosenberg, K. Petrukhin, and C. Wadelius. 1999. The mutation spectrum of the bestrophin protein-functional implications. *Hum. Genet.* 104:383–389.

Bakall, B., L.Y. Marmorstein, G. Hoppe, N.S. Peachey, C. Wadelius, and A.D. Marmorstein. 2003. Expression and localization of bestrophin during normal mouse development. *Invest. Ophthalmol. Vis. Sci.* 44:3622–3628.

Bialek, S., D.P. Joseph, and S.S. Miller. 1995. The delayed basolateral membrane hyperpolarization of the bovine retinal pigment epithelium: mechanism of generation. *J. Physiol.* 484:53–67.

Caldwell, G.M., L.E. Kakuk, I.B. Griesinger, S.A. Simpson, N.J. Nowak, K.W. Small, I.H. Maumenee, P.J. Rosenfeld, P.A. Sieving, T.B. Shows, and R. Ayyagari. 1999. Bestrophin gene mutations in patients with Best vitelliform macular dystrophy. *Genomics.* 58:98–101.

Dascal, N. 1997. Signalling via the G protein-activated K^+ channels. *Cell. Signal.* 9:551–573.

Deutman, A.F. 1969. Electro-oculography in families with vitelliform dystrophy of the fovea. Detection of the carrier state. *Arch. Ophthalmol.* 81:305–316.

Doyle, D.A., J.M. Cabral, R.A. Pfuetzner, A. Kuo, J.M. Gulbis, S.L. Cohen, B.T. Chait, and R. MacKinnon. 1998. The structure of the potassium channel: molecular basis of K^+ conduction and selectivity. *Science.* 280:69–77.

Dutzler, R., E.B. Campbell, M. Cadene, B.T. Chait, and R. MacKinnon. 2002. X-ray structure of a ClC chloride channel at 3.0 A reveals the molecular basis of anion selectivity. *Nature.* 415:287–294.

Dutzler, R., E.B. Campbell, and R. MacKinnon. 2003. Gating the selectivity filter in ClC chloride channels. *Science.* 300:108–112.

Eisenman, G., and R. Horn. 1983. Ionic selectivity revisited: the role of kinetic and equilibrium processes in ion permeation through channels. *J. Membr. Biol.* 76:197–225.

Elble, R.C., G. Ji, K. Nehrke, J. DeBiasio, P.D. Kingsley, M.I. Kotlikoff, and B.U. Pauli. 2002. Molecular and functional characterization of a murine calcium-activated chloride channel expressed in smooth muscle. *J. Biol. Chem.* 277:18586–18591.

Faundez, V., and H.C. Hartzell. 2004. Intracellular chloride channels: determinants of function in the endosomal pathway. *Sci. STKE.* In press.

Francois, J., A. De Rouck, and D. Fernandez-Sasso. 1967. Electro-oculography in vitelliform degeneration of the macula. *Arch. Ophthalmol.* 77:726–733.

Fujii, S., R.P. Gallemore, B.A. Hughes, and R.H. Steinberg. 1992. Direct evidence for a basolateral membrane Cl^- conductance in toad retinal pigment epithelium. *Am. J. Physiol.* 262:C374–C383.

Fuller, C.M., and D.J. Benos. 2000. Electrophysiological characteristics of the Ca^{2+}-activated Cl^- channel family of anion transport proteins. *Clin. Exp. Pharmacol. Physiol.* 27:906–910.

Gallemore, R.P., B.A. Hughes, and S.S. Miller. 1998. Transport mechanisms in the retinal pigment epithelium. *In* The Retinal Pigment Epithelium. M.F. Marmor and T.J. Wolfensberger, editors. Oxford University Press, Oxford. 175–198.

Gallemore, R.P., and R.H. Steinberg. 1993. Light-evoked modulation of basolateral membrane Cl^- conductance in chick retinal pigment epithelium: the light peak and fast oscillation. *J. Neurophysiol.* 70:1669–1680.

Gass, J.D.M. 1987. Stereoscopic Atlas of Macular Diseases: Diagnosis and Treatment. C.V. Mosby & Co., St. Louis, MO.

Griff, E.R. 1991. Potassium-evoked responses from the retinal pigment epithelium of the toad *Bufo marinus*. *Exp. Eye Res.* 53:219–228.

Isomoto, S., C. Kondo, and Y. Kurachi. 1997. Inwardly rectifying potassium channels: their molecular heterogeneity and function. *Jpn. J. Physiol.* 47:11–39.

Jentsch, T.J., V. Stein, F. Weinreich, and A.A. Zdebik. 2002. Molecular structure and physiological function of chloride channels. *Physiol. Rev.* 82:503–568.

Ji, H.-L., M.D. DuVall, H.K. Patton, C.L. Satterfield, C.M. Fuller, and D.J. Benos. 1998. Functional expression of a truncated Ca^{2+}-activated Cl^- channel and activation by phorbol ester. *Am. J. Physiol.* 274:C455–C464.

Karlin, A., and M.H. Akabas. 1998. Substituted-cysteine accessibility method. *Methods Enyzmol.* 293:123–145.

Kirsch, G.E., J.A. Drewe, M. Taglialatela, R.H. Joho, M. DeBiasi, H.A. Hartmann, and A.M. Brown. 1992. A single nonpolar residue in the deep pore of related K^+ channels acts as a K^+:Rb^+ conductance switch. *Biophys. J.* 62:136–143.

Kuruma, A., and H.C. Hartzell. 2000. Bimodal control of a Ca^{2+}-activated Cl^- channel by different Ca^{2+} signals. *J. Gen. Physiol.* 115:59–80.

Kuruma, A., Y. Hirayama, and H.C. Hartzell. 2000. A hyperpolarization- and acid-activated nonselective cation current in Xenopus oocytes. *Am. J. Physiol. Cell Physiol.* 279:C1401–C1413.

Linsdell, P. 2001. Thiocyanate as a probe of the cystic fibrosis transmembrane conductance regulator chloride channel pore. *Can. J. Physiol. Pharmacol.* 79:573–579.

Loewen, M.E., L.K. Bekar, S.E. Gabriel, W. Walz, and G.W. Forsyth. 2002a. pCLCA1 becomes a cAMP-dependent chloride conductance mediator in Caco-2 cells. *Biochem. Biophys. Res. Commun.* 298:531–536.

Loewen, M.E., S.E. Gabriel, and G.W. Forsyth. 2002b. The calcium-dependent chloride conductance mediator pCLCA1. *Am. J. Physiol. Cell Physiol.* 283:C412–C421.

Machaca, K., Z. Qu, A. Kuruma, H.C. Hartzell, and N. McCarty. 2002. The endogenous calcium-activated Cl channel in *Xenopus* oocytes: a physiologically and biophysically rich model system. *In* Calcium-activated Chloride Channels. C.M. Fuller, editor. Academic Press, San Diego. 3–39.

Mansoura, M.K., S.S. Smith, A.D. Choi, N.W. Richards, T.V. Strong, M.L. Drumm, F.S. Collins, and D.C. Dawson. 1998. Cystic fibrosis transmemebrane conductance regulator (CFTR) anion binding as a probe of the pore. *Biophys. J.* 74:1320–1332.

Marmorstein, A.D., L.Y. Mormorstein, M. Rayborn, X. Wang, J.G. Hollyfield, and K. Petrukhin. 2000. Bestrophin, the product of the Best vitelliform macular dystrophy gene (VMD2), localizes to the basolateral membrane of the retinal pigment epithelium.

Proc. Natl. Acad. Sci. USA. 97:12758–12763.

O'Gorman, S., W.A. Flaherty, G.A. Fishman, and E.L. Berson. 1988. Histopathologic findings in Best's vitelliform macular dystrophy. *Arch. Ophthalmol.* 106:1261–1268.

Papassotiriou, J., J. Eggermont, G. Droogmans, and B. Nilius. 2001. Ca^{2+}-activated Cl^- channels in Ehrlich ascites tumor cells are distinct from mCLCA1, 2 and 3. *Pflugers Arch.* 442:273–279.

Petrukhin, K., M.J. Koisti, B. Bakall, W. Li, G. Xie, T. Marknell, O. Sandgren, K. Forsman, G. Holmgren, S. Andreasson, et al. 1998. Identification of the gene responsible for Best macular dystrophy. *Nat. Genet.* 19:241–247.

Qu, Z., and H.C. Hartzell. 2000. Anion permeation in Ca-activated Cl channels. *J. Gen. Physiol.* 116:825–844.

Qu, Z., and H.C. Hartzell. 2001. Functional geometry of the permeation pathway of Ca^{2+} activated Cl^- channels in ferred from analysis of voltage-dependent block. *J. Biol. Chem.* 276:18423–18429.

Qu, Z., and H.C. Hartzell. 2003. Two bestrophins cloned from *Xenopus laevis* oocytes express Ca-activated Cl currents. *J. Biol. Chem.* 278:49563–49572.

Smith, S.S., E.D. Steinle, M.E. Meyerhoff, and D.C. Dawson. 1999. Cystic fibrosis transmembrane conductance regulator: physical basis for lyotropic anion selectivity patterns. *J. Gen. Physiol.* 114: 799–817.

Steinberg, R.H. 1985. Interactions between the retinal pigment epithelium and the neural retina. *Doc. Ophthalmol.* 60:327–346.

Stohr, H., A. Marquardt, I. Nanda, M. Schmid, and B.H. Weber. 2002. Three novel human VMD2-like genes are members of the evolutionary highly conserved RFP-TM family. *Eur. J. Hum. Genet.* 10:281–284.

Sun, H., T. Tsunenari, K.-W. Yau, and J. Nathans. 2002. The vitelliform macular dystrophy protein defines a new family of chloride channels. *Proc. Natl. Acad. Sci. USA.* 99:4008–4013.

Taglialatela, M., J.A. Drewe, G.E. Kirsch, M. De Biasi, H.A. Hartmann, and A.M. Brown. 1993. Regulation of K^+/Rb^+ selectivity and internal TEA blockade by mutations at a single site in K^+ pores. *Pflugers Arch.* 423:104–112.

Tsien, R.Y., and T. Pozzan. 1989. Measurements of cytosolic free Ca^{2+} with Quin-2. *Methods Enzymol.* 172:230–262.

Tsunenari, T., H. Sun, J. Williams, H. Cahill, P. Smallwood, K.-W. Yau, and J. Nathans. 2003. Structure-function analysis of the bestrophin family of anion channels. *J. Biol. Chem.* 278:41114–41125.

White, K., A. Marquardt, and B.H.F. Weber. 2000. VMD2 mutations in vitelliform macular dystrophy (Best disease) and other maculopathies. *Hum. Mutat.* 15:301–308.

Zhou, Y., J.H. Morais-Cabral, A. Kaufman, and R. MacKinnon. 2001. Chemistry of ion coordination and hydration revealed by a K^+ channel-Fab complex at 2.0 A resolution. *Nature.* 414:43–48.